Extremely Complex Populations of Small RNAs in the Mouse Retina and RPE/Choroid

Sudha Priya Soundara Pandi, Mei Chen, Jasenka Guduric-Fuchs, Heping Xu, and David Arthur Simpson

Centre for Vision and Vascular Science, Queen's University Belfast, Belfast, Northern Ireland, United Kingdom

Correspondence: David Arthur Simpson, Queen's University Belfast Centre for Experimental Medicine, Institute of Clinical Science A, Royal Victoria Hospital, Belfast, BT12 6BA, Northern Ireland, UK; David.Simpson@qub.ac.uk.

Submitted: June 19, 2013
Accepted: November 3, 2013

Citation: Soundara Pandi SP, Chen M, Guduric-Fuchs J, Xu H, Simpson DA. Extremely complex populations of small RNAs in the mouse retina and RPE/choroid. *Invest Ophthalmol Vis Sci*. 2013;54:8140–8151. DOI:10.1167/iovs.13-12631

Purpose. MicroRNAs (miRNAs) are small noncoding RNAs of approximately 18 to 22 nucleotides in length that regulate gene expression. They are widely expressed in the retina, being both required for its normal development and perturbed in disease. The aim of this study was to apply new high-throughput sequencing techniques to more fully characterize the miRNAs and other small RNAs expressed in the retina and retinal pigment epithelium (RPE)/choroid of the mouse.

Methods. Retina and RPE/choroid were dissected from eyes of 3-month-old C57BL/6J mice. Small RNA libraries were prepared and deep sequencing performed on a genome analyzer. Reads were annotated by alignment to miRBase, other noncoding RNA databases, and the mouse genome.

Results. Annotation of 9 million reads to 320 miRNAs in retina and 340 in RPE/choroid provides the most comprehensive profiling of miRNAs to date. Two novel miRNAs were identified in retina. Members of the sensory organ–specific miR-183, -182, -96 cluster were among the most highly expressed, retina-enriched miRNAs. Remarkably, miRNA "isomiRs," which vary slightly in length and are differentially detected by Taqman RT-qPCR assays, existed for all the microRNAs identified in both tissues. More variation occurred at the 3′ ends, including nontemplated additions of T and A. Drosha-independent mirtron miRNAs and other small RNAs derived from snoRNAs were also detected.

Conclusions. Deep sequencing has revealed the complexity of small RNA expression in the mouse retina and RPE/choroid. This knowledge will improve the design and interpretation of future functional studies of the role of miRNAs and other small RNAs in retinal disease.

Keywords: microRNA, retina, RPE, miRNA, RNA-Seq

MicroRNAs are small noncoding RNAs of approximately 18 to 22 nucleotides in length that regulate gene expression[1] and play critical roles in development, homeostasis, and pathogenesis[2] of the retina. Their function in retinal development was first suggested by the distinctive temporal and spatial expression patterns observed for specific microRNAs.[3–7] This was confirmed by the perturbed differentiation, severe malformation, and subsequent degeneration of the retina[8–10] observed in mouse models in which Dicer, an RNase III endonuclease required for the biogenesis of most microRNAs, was conditionally knocked out in the retina. The functions of some individual microRNAs have been elucidated. For example, miR-24a negatively regulates apoptosis during development of the retina in *Xenopus*.[11] Two microRNAs highly expressed in the adult RPE, miR-204 and miR-211, have been demonstrated to promote RPE differentiation.[12,13]

Expression of the miR-183/96/182 "sensory-organ–specific" microRNA cluster increases during retinal development and peaks in the adult photoreceptors (and certain ganglion cells), suggesting a role in the normal functioning of the adult retina.[7,14] Indeed, knockout of the miR-183 cluster results in defects in the ERG and progressive retinal degeneration.[14] The characteristic changes in microRNA expression observed in animal models of retinal degeneration[15] are consistent with the wider involvement of microRNAs in this process. The microRNAs of the miR-183 cluster are among several that are regulated by light and mediate circadian responses.[7,16]

microRNAs also have been associated with retinal vascular function. In a mouse model of ocular neovascularization, the levels of three microRNAs were significantly decreased (miR-31, -150, and -184), and it was shown that supplementation of these microRNAs could reduce the neovascular response.[17] miR-23 and miR-27 modulate retinal vascular development and their inhibition can repress laser-induced choroidal neovascularization.[18,19]

Most studies of the retina to date have focused on individual or groups of microRNAs, as defined by the canonical sequences registered in miRBase.[20] However, each microRNA actually comprises a family of sequences differing by several nucleotides at either end. These variants or "isomiRs" originate during microRNA biogenesis (Fig. 1). MicroRNAs are transcribed by RNA polymerase II[21] as independent transcripts or are located within introns of coding genes. These primary transcripts (pri-microRNAs) are processed by the RNaseIII enzyme Drosha to form approximately 70 nt stem-loop "pre-microRNAs"[22] with 5p and 3p arms and two nucleotide unpaired 3′ tails, which are transported from the nucleus to the cytoplasm by exportin-5. Here they are processed by another RNaseIII enzyme, Dicer, to form short duplexes, which may undergo further modifications. One strand (this is predominantly either the 5p or 3p,

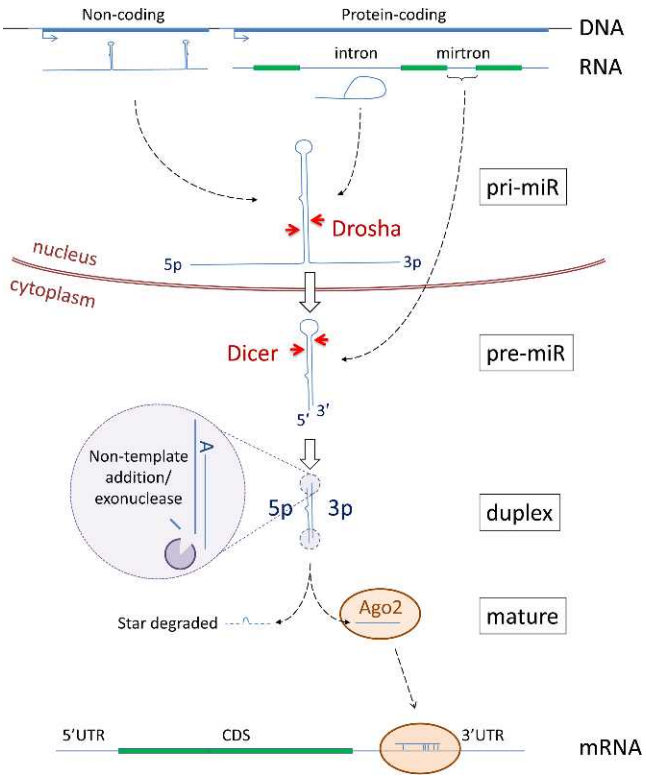

Figure 1. MicroRNA biogenesis. MicroRNAs can be either transcribed as independent transcripts or located within introns of protein-coding genes. In the canonical pathway, the primary transcript (pri-miR) forms a stem loop structure which is cleaved by the RNaseIII enzyme Drosha to form a pre-miR. This is exported to the cytoplasm where it is cleaved by another RNaseIII enzyme, Dicer, to form a duplex comprising one strand from the 5p arm of the pre-miR and one from the 3p arm. There can be some variation in the lengths of the strands due to differential cleavage or nontemplated addition of ribonucleotides; this is the source of isomiRs. One strand of the duplex is incorporated into the RISC complex to become the mature microRNA, which directs inhibition of target genes via partially complementary target sites in their 3′ UTRs. The other strand, referred to as the "star" sequence is degraded. The mature microRNA is often predominantly from one arm of the pre-miR, but the proportion of 5p and 3p can vary.

depending on the specific microRNA) is then loaded into the RNA-induced silencing complex (RISC), which comprises Argonaute proteins and other accessory factors. In contrast to the other strand, which is degraded, the mature microRNA directs RISC-mediated inhibition of translation or degradation of mRNA targets, as determined by incomplete complementary base pairing.

Each microRNA gene can therefore give rise to multiple mature microRNA isomiRs, which vary slightly in length or sequence due to differential processing. It is important to investigate isomiRs, because they can have different activities[23] and stability.[24] The most commonly used techniques for studying microRNA expression, RT-PCR and microarrays, often detect a single canonical isomiR of each microRNA or do not discriminate between isomiRs. However, "next-generation" sequencing (NGS) approaches can provide the individual sequences of millions of cloned microRNAs in parallel.[25] In addition to individual isomiRs, microRNAs derived from both arms of the pre-miR (with different target genes) and any other small RNAs of a similar size are detected by this "RNA-Seq" technology.

The aim of this study was to employ RNA-Seq to define the complement of small RNAs expressed in the adult retina and RPE/choroid. This revealed that each tissue contains a characteristic profile of known and novel small RNAs, both in terms of absolute expression and isomiR profiles. The breadth of microRNA interactions within the retina is likely to be even more complicated than suggested by the studies of canonical microRNAs to date.

Methods

Samples

C57BL/6J mice were housed in a standard experimental room and exposed to a 12 hour:12 hour light-dark cycle. All the procedures were carried out in compliance with the ARVO statement for the Use of Animals in Ophthalmic and Vision Research, and under the regulations of the Animals (Scientific Procedures) Act 1986 (UK).

Sample Collection

Retina ($n = 3$) and RPE/choroidal ($n = 2$) tissues were collected from 3-month-old C57BL/6J mice. The animals were killed with CO_2 inhalation; eyes were enucleated; cornea, iris, ciliary body, and lens were removed; and retina was peeled off and separated from RPE/choroid within 5 minutes. The retina and RPE/choroid samples were immediately transferred to RNA lysis buffer (Qiazol; Qiagen, Manchester, UK), snap frozen with liquid nitrogen, and stored at −80°C for the total RNA extraction.

RNA Extraction and Quality Control

Total RNA was extracted from retina and RPE/choroid samples using a microRNeasy Kit (Qiagen) following the manufacturer's instructions. RNA was quantified using a NanoDrop ND-1000 spectrophotometer (NanoDrop Technologies, Wilmington, DE) and the integrity evaluated using an RNA 6000 Nano chip on a Bioanalyzer (Agilent Technologies, Wokingham, UK); only samples with an RNA integrity number (RIN) higher than 8.0 were used for library preparation.

Polyadenylation and Reverse Transcription Quantitative Polymerase Chain Reaction (qPCR)

RT-qPCR was performed using a modified version of the method described by Shi and Chiang,[26] whereby mature microRNAs are polyadenylated and target sequences for a reverse primer are subsequently incorporated into cDNA by use of an oligo dT adapter. One microgram of total RNA was polyadenylated using Poly(A) polymerase (PAP; Life Technologies, Paisley, UK) in a 25 μL reaction mix at 37°C for 1 hour in a thermocycler. The polyadenylated RNAs were then reverse transcribed with 200 U reverse transcriptase (SuperScript III; Life Technologies) and 0.5 ng poly (T) adapter (3′rapid amplification of complementary DNA ends [RACE] adapter in the FirstChoice RLM-RACE kit; Ambion, Paisley, UK).

Primers for specific microRNAs were designed that were shorter than the canonical mature sequence to facilitate amplification of all the abundant isomiRs identified by deep sequencing. The reverse primer was the 3′adapter primer (3′RACE outer primer). PCR was performed for 45 cycles with denaturation at 94°C for 30 seconds, annealing at 60°C for 30 seconds, and extension at 72°C for 30 seconds (LightCycler 480; Roche, Mannheim, Germany). The primer sequences are listed in Supplementary Table S1. The RT-qPCR data were analyzed using REST 2009 software (Qiagen).[27]

Investigative Ophthalmology & Visual Science

Table 1. Annotation Report of the Retina and RPE/Choroid Libraries

Library*	Raw Reads	Reads After Adapter Trimming	Average Length of Sequence	Reads Annotated With miRBase -V.18.0 (%)	Unique Reads	Unique Reads Annotated With miRBase	No. of Pre-miR		
							Mature From 5p (%)	Mature From 3p (%)	Total
Retina									
RET 1	2,047,447	1,822,622	21.8	1,723,849 (91.5)	54,402	15,720	193 (46)	223 (54)	417
RET 2	1,449,040	1,337,687	21.7	1,254,794 (93.8)	38,386	12,544	187 (49)	198 (51)	385
RET 3	1,192,071	984,981	21.8	927,539 (94.1)	31,489	10,970	180 (47)	202 (53)	382
RPE/Choroid									
R/C 1	3,886,781	3,687,115	23.9	2,808,481 (76.1)	212,322	25,581	229 (49)	237 (51)	466
R/C 2	3,681,869	3,491,303	24.8	2,365,902 (67.7)	221,368	24,051	237 (51)	230 (49)	467

* RET1-3 and R/C1-2 refer to individual retinal and RPE/choroid small RNA libraries, respectively.

The expression of miR-127 and its isomiR were analyzed using a Taqman microRNA assay for the mature canonical miR-127-3p (UCGGAUCCGUCUGAGCUUGGCU) and a custom Taqman small RNA assay (assay ID CSX0ZZO) for the miR-127 3′ isomiR (UCGGAUCCGUCUGAGCUUGG; Life Technologies). Reverse transcription and PCR were performed according to the manufacturer's instructions.

cDNA Library Construction and Deep Sequencing

Small RNA libraries were constructed using a Truseq small RNA sample preparation kit (Illumina, San Diego, CA) following the manufacturer′s protocol. Briefly, 3′ and 5′ adapters were ligated to small RNA, followed by reverse transcription, PCR amplification with index sequences specific for each sample, and purification from 6% polyacrylamide gel of 147- to 157-bp products from pooled indexes. Libraries were validated using a DNA 1000 chip on a Bioanalyzer (Agilent Technologies). Cluster generation and sequencing on a Genome Analyzer II (Illumina) was performed at the Trinity Genome Sequencing Laboratory, Dublin (http://www.medicine.tcd.ie/sequencing).

Data Analysis

The adapter sequences were trimmed and reads aligned to mouse microRNAs in the miRBase database (Release 18.0)[20] using Genomics Workbench V4.0 software (CLCbio, Aarhus, Denmark), allowing two mismatches. The number of reads for each microRNA were normalized to reads per million mapped (RPM). The reads that did not match any annotated mouse microRNAs were aligned with other mammalian microRNAs to identify potential novel orthologs. To confirm that matching sequences represented novel orthologs, their genomic location and secondary structure were investigated using the UCSC genome browser (http://genome.ucsc.edu) and RNA fold WebServer (http://rna.tbi.univie.ac.at/cgi-bin/RNAfold.cgi). En-

Table 2. The 10 Most Highly Expressed microRNAs in Retina and RPE/Choroid

Name	C57BL6 Normalized Mean Expression Values, (RPM)	Ratio of Retina and RPE/Choroid Normalized Mean	Ratio of RPE/Choroid and Retina Normalized Mean	Localization by ISH*
Retina				
miR-182-5p	385,280 (±50272)	**94.9**		GCL, INL, ONL, PHOT[4,5,7]
miR-183-5p	139,435 (±35988)	**104.1**		GCL, INL, ONL, PHOT[4,5,7]
miR-181a-5p	124,750 (±23969)	**5.2**		GCL, INL[4,5]
miR-26a-5p	29,022 (±4158)	0.3		—
miR-127-3p	24,017 (±3458)	3.5		GCL, INL ONL, PHOT, RPE[4,5]
miR-204-5p	20,101 (±726)	0.3		INL[4,5] RPE[55]
miR-125a-5p	15,818 (±6047)	0.5		—
miR-99b-5p	15,532 (±3401)	0.8		INL, PHOT[4,5]
miR-30d-5p	14,956 (±3840)	0.7		GCL, INL, PHOT, RPE[4,5]
miR-211-5p	13,950 (±582)	0.8		—
RPE/Choroid				
miR-143-3p	105,258 (±7505)		**30.3**	IR[4,5]
miR-22-3p	99,317 (±6027)		**9.8**	—
miR-26a-5p	90,849 (±8064)		3.1	—
miR-204-5p	66,569 (±2178)		3.3	INL[4,5]RPE[55]
miR-133a-3p	51,214 (±3249)		**1164.9**	—
miR-27b-3p	46,840 (±2837)		**6.2**	—
miR-125a-5p	32,443 (±2181)		2.1	—
miR-30a-5p	30,652 (±626)		2.2	GCL, INL[4,5]
miR-30d-5p	20,033 (±1686)		1.3	GCL, INL, PHOT, RPE[4,5]
miR-99b-5p	19,312 (±3595)		1.2	INL, PHOT[4,5]

MicroRNAs highly enriched in either retina or RPE/choroid are indicated in bold. GCL, ganglion cell layer; INL, inner nuclear layer; IR, iris; ONL, outer nuclear layer; PHOT, photoreceptor; —, no localization information available.

* Numbers refer to references.

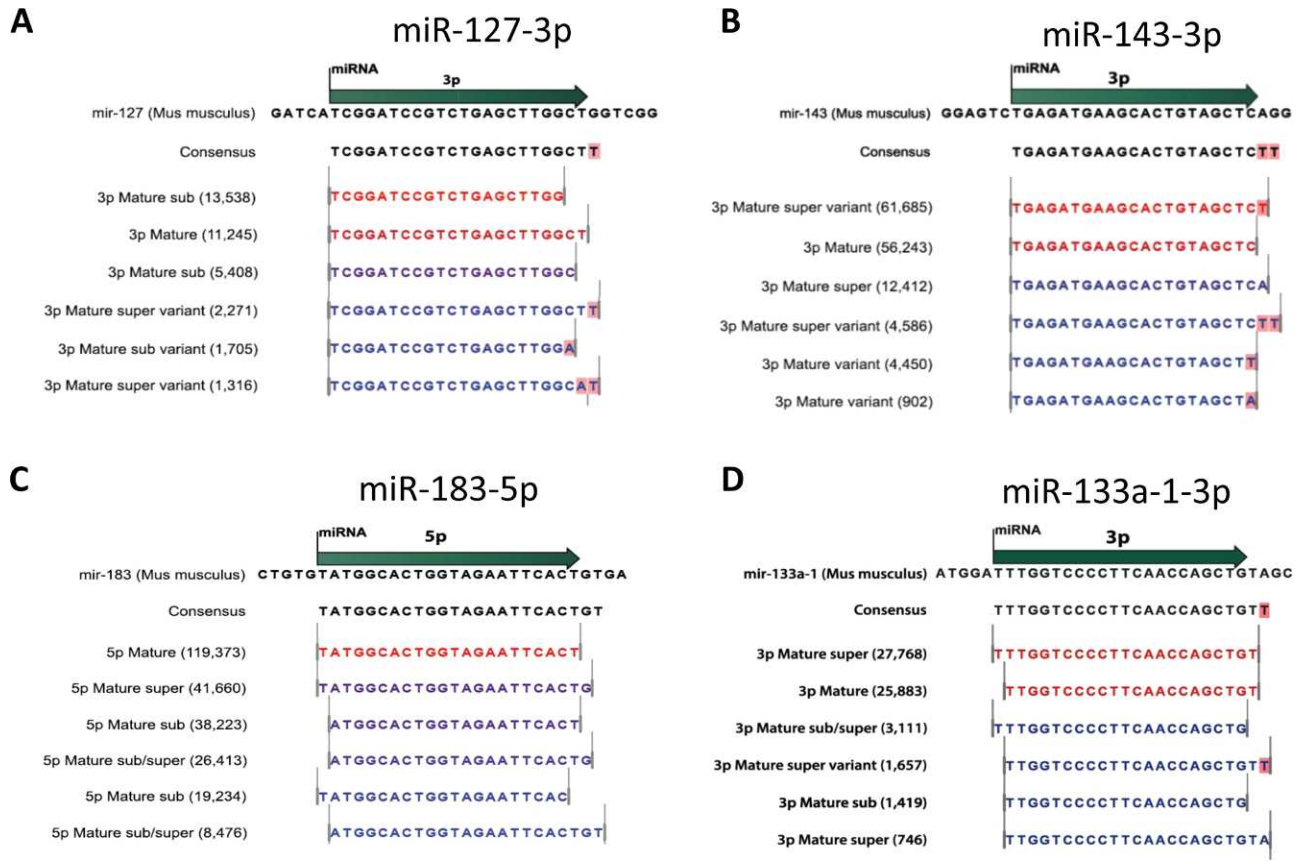

Figure 2. microRNA isomiRs. (**A**) miR-127-3p was highly expressed in the retina and exhibited many isomiRs at the 3′ end, with the most common sequence observed being shorter than the mature sequence present in miRBase. IsomiRs with nontemplated addition of both A and T nucleotides were present. (**B**) miR-143-3p was highly expressed in RPE/choroid and exhibited many isomiRs at the 3′ end. The most common sequence observed was one nucleotide longer than the mature sequence present in miRBase due to nontemplated addition of a T nucleotide. (**C**) The most highly expressed microRNA in retina, miR-183-5p, showed both 5′ and 3′ isomiRs. One-third of all mature miR-183 reads were one nucleotide shorter at the 5′ end than the canonical sequence. (**D**) Both 5′ and 3′ isomiRs were also detected for miR-133a-1-3p.

semble noncoding RNA annotations, including small nucleolar RNAs (snoRNAs), for the mouse genome were downloaded using Biomart (www.biomart.org). For the identification of putative novel microRNAs, the unannotated unique sequences were converted into FASTA format using "FASTA manipulation" in the Galaxy Web-based platform (https://main.g2.bx.psu.edu) and submitted to mirTools Web server (http://centre.bioinformatics.zj.cn/mirtools/).[28] The genomic location and potential secondary structure of putative novel microRNA sequences were assessed as for novel orthologs above. Publicly available small RNA sequencing data from a range of mouse tissues were accessed via the Gene Expression Omnibus database (GEO),[29] to analyze the expression level of novel microRNAs in other mouse tissues. Reads were mapped to mirtron sequences downloaded from the Eric Lai lab (http://ericlailab.com/mammalian_mirtrons/mm9/).[30] The predicted targets and involvement in signaling pathways of the highly expressed retina- and RPE/choroid-enriched microRNAs were analyzed using DIANA miRPath V2.0,[31] and the predicted targets for isomiRs analyzed using DIANA microT V3.0.[32]

Results

Sequencing Data and Mapping

Deep sequencing generated an average of 2.5 million reads from each of the retinal or RPE/choroidal small RNA libraries (Table 1). Following adapter trimming, most reads were in the range of 20 to 24 bp, as expected for microRNAs (Supplementary Fig. S1A). Mapping to miRBase revealed the presence of microRNAs derived from 320 and 340 pre-miRs from retina and RPE respectively, when considering only microRNAs with more than 5 reads as expressed. The number of reads for each of the microRNAs was normalized to reads per million mapped and the mean expression values from replicate libraries in the retina and RPE/choroid were calculated (Supplementary Tables S2A, S2B). The 10 most highly expressed microRNAs in retina and RPE/choroid are listed in Table 2. Although some microRNAs, such as miR-99b-5p and miR-30d-5p, were expressed at similar levels, others were highly enriched in either the RPE/choroid (e.g., miR-133a-3p [1164x], miR-143-3p [30x] miR-22-3p [10x] and miR-27b-3p [6x]) or the retina (e.g., miR-182-5p [95x], miR-183-5p [104x], miR-181a-5p [5x]; Table 2). The relative expression of the highly expressed microRNAs that showed the greatest variations between retina and RPE was independently validated by SYBR green RT-qPCR (which amplifies all isomiRs). This confirmed the pattern of expression both in the samples used for deep sequencing and in an additional group of biological replicates (Supplementary Fig. S2).

IsomiRs and IsomoRs

Each microRNA is not represented by a single sequence but by a series of "isomiRs." These vary both at the 5′ and more

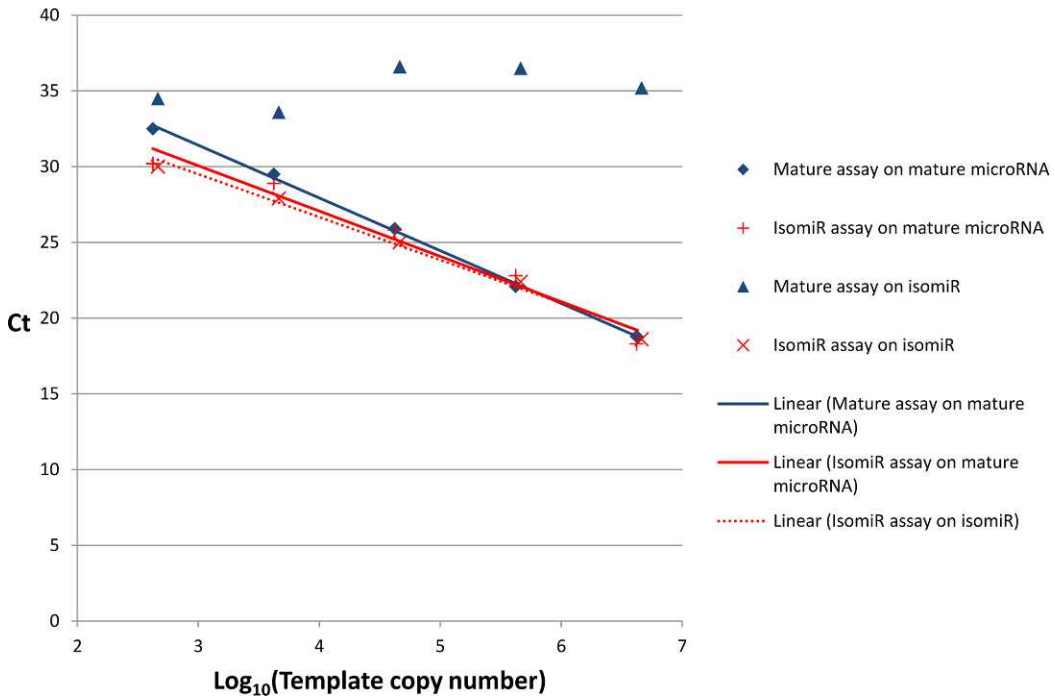

FIGURE 3. Taqman RT-qPCR of miR-127-3p mature and 3′ isomiR sequences. A Taqman assay for miR-127-3p (mature assay) and a custom small RNA Taqman assay targeting the 3′ isomiR were used to quantify dilution series of either the mature microRNA (*solid line*) or the isomiR (*dotted line*). Although the mature assay was specific for the mature sequence (only nonspecific products detected at high Ct values that did not correlate with template concentration were amplified from the isomiR sequence), the isomiR assay amplified both the isomiR and mature sequences with similar efficiency (*red lines*).

frequently at the 3′ end due to differential cleavage by Drosha or Dicer and/or subsequent processing, such as nontemplate additions catalyzed by nucleotidyl transferase enzymes[33] (Fig. 1). Although one canonical sequence often predominates, all the microRNAs detected exhibited isomiRs and in many cases they represented a significant proportion of all reads. There were many cases in which the most frequent isomiR was not the canonical mature sequence defined in miRBase, for example miR-127-3p and miR-143-3p (Figs. 2A, 2B).

The presence of abundant isomiRs could confound assays that target specific sequences, such as the widely used Taqman microRNA arrays. We therefore tested the ability of a Taqman assay for the canonical mature sequence from miRBase and a custom Taqman small RNA assay designed to target the 3′ isomiR of miR-127-3p, to amplify synthetic microRNA sequences mimicking the mature and isomiR sequences. Although the mature miR-127-3p assay was specific for the mature microRNA, the isomiR assay detected both the isomiR and the mature microRNA with similar efficiency (Fig. 3). The deep sequencing data indicated that the miR-127-3p mature and isomiR sequences are present at similar levels in the retina (Fig. 2A). Consistent with its ability to amplify both miR-127-3p sequences, the Ct value for amplification from retinal cDNA of the miR-127-3p isomiR assay was consistently one cycle earlier than that for the mature assay (0.96 ± 0.23; $n = 4$). The Taqman miR-127-3p assay therefore underestimates the total amount of miR-127-3p present in the tissue.

The seed region of microRNA (nucleotides 2–8) is the main determinant of target selection.[34] IsomiRs that vary at the 5′ end have different seed sequences and therefore have the greatest potential functional significance. Many 5′ isomiRs were observed in both retina and RPE/choroid. For example, the second most abundant microRNA in retina, miR-183-5p, expressed several isomiRs lacking one base at the 5′ end, presumably due to differential cleavage by Drosha and comprising a quarter of all reads (Fig. 2C). More 5′ isomiRs were observed for microRNAs derived from the 3p arm, possibly due to differential cleavage by Dicer, for example miR-133a-1 (Fig. 2D). Some microRNAs, including miR-124, are encoded by more than one gene and isomiRs may be generated by different processing of the alternative pri- and pre-miRs.

Frequent nontemplated additions were observed at the 3′ ends of most microRNAs in both retina and RPE/choroid. These were most frequently A or T nucleotides, which is in agreement with previous reports.[25,35–37] For example, miR-143-3p exhibited both an additional T in the most frequent isomiR and an additional A in a minor isomiR (Fig. 2B).

It was notable that the pattern of relative expression of the isomiRs of a specific microRNA was very consistent between the retinal samples, but distinct from a different, but equally consistent expression pattern observed in the RPE/choroid. This was true for most microRNAs and is vividly demonstrated by miR-182-5p (Supplementary Fig. S3). MicroRNA offset RNAs (IsomoRs) are short RNAs derived from the regions adjacent to the mature and mature star microRNAs. They are by-products generated during microRNA processing and their functional significance is unclear.[38–40] IsomoRs were detected for eight microRNAs in retina and six in RPE/choroid. These were mostly 5′ isomoRs that clearly define the 5′ end of the mature microRNA, as illustrated by miR-96 in the retina and miR-211 in the RPE/choroid (Fig. 4).

Arm Selection of Mature microRNAs

The mature microRNA strand is selected from either the 5p or 3p arm (the choice at least partly depending on the thermodynamic stability of the duplex end[41]) and loaded into an Argonaute protein, while the other "star" strand is degraded

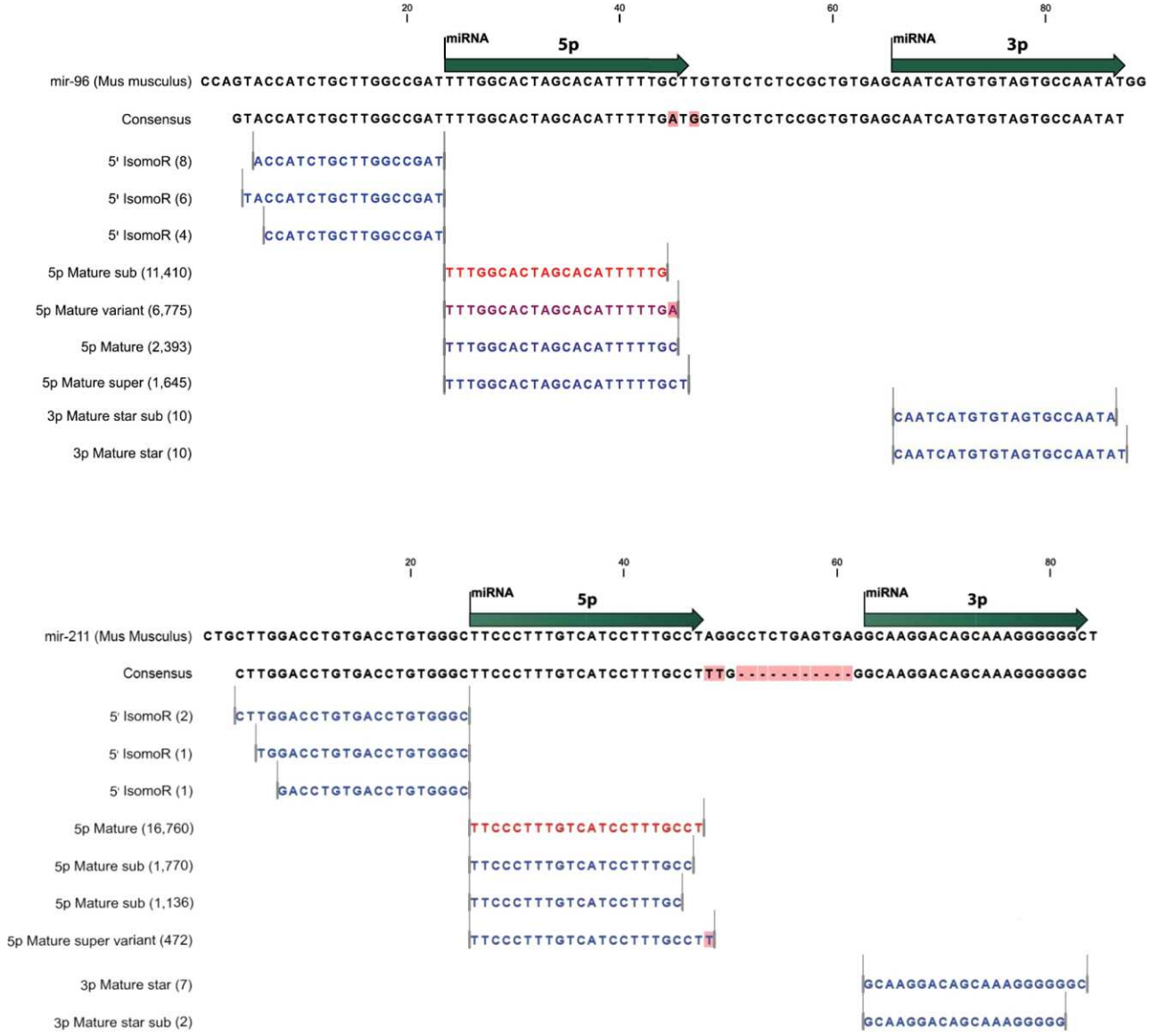

Figure 4. Offset microRNAs (isomoRs). These are generated during microRNA biogenesis and define the ends of the mature microRNAs. We observed 5′ isomoRs in both the retina (e.g., miR-96-5p; *top panel*) and in the RPE/choroid (e.g., miR-211-5p; *bottom panel*). Both microRNAs exhibited 3′ isomiRs, including nontemplated additions.

(Fig. 1). For many microRNAs, one mature strand predominates. For both retina and RPE/choroid, similar numbers of mature microRNAs from each arm were detected (retina 47% 5p and 53% 3p; RPE/choroid, 50% from each arm). We then analyzed the ratios of 5p to 3p sequences for each of the individual microRNAs. For most of those expressed in both retina and RPE/choroid, the 5p:3p ratio was similar (Fig. 5), but some exhibited significant changes in the proportion of sequences from each arm. For example, miR-151 and miR-345 exhibited arm switching (i.e., the most common mature sequence was derived from alternate arms in retina and RPE/choroid). Some highly expressed microRNAs had a large number of sequences derived from both arms; for example, miR-126 had an average of 11,678 RPM from 5p and 5728 RPM from 3p and miR-145 had an average of 935 RPM from 5p and 961 RPM from 3p in the RPE. In both of these cases, the most abundant sequences are from the opposite arm to that considered to be the canonical mature microRNA in miRBase and would therefore not be assessed by many assays based on this annotation. The arm selection of miR-126 was particularly notable because in other mouse tissues and almost all other species present in miRBase, the mature microRNA is derived from the 3p arm.

In general, much greater numbers of sequences were detected from one arm than the other of each microRNA, presumably reflecting preferential loading into RISC. Remarkably, the more highly expressed microRNAs tended to be generated even more predominantly from one arm than the lower expressed microRNAs, which exhibited less extreme ratios between the numbers of reads from 5p and 3p arms (Fig. 5).

Other Small RNAs

Although the majority of all reads (81%) mapped to known microRNAs, there was a wide range of other RNAs detected: 12% of unique reads mapped to other noncoding and 12% to repeat-associated RNAs, although these each represented only

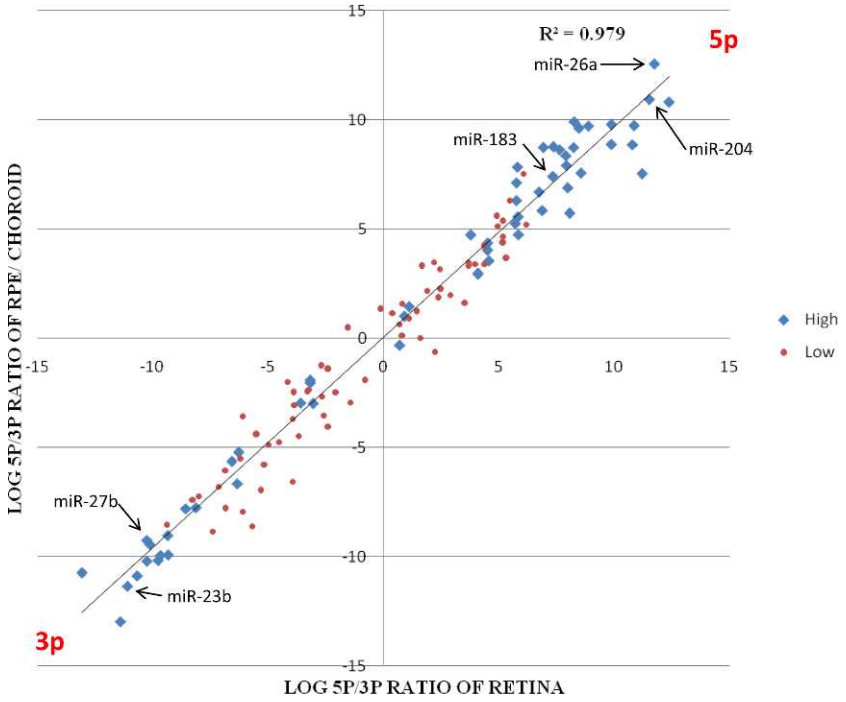

Figure 5. Ratios of mature microRNAs derived from 5p and 3p pre-miR arms. For all microRNAs represented by more than 20 RPM, the ratios of the numbers of reads derived from the 5p and 3p arms were calculated. A plot of the $\log_2$ values of the 5p:3p ratios from retina against those from RPE/choroid demonstrated that the ratios were generally highly conserved ($R^2 = 0.966$), although there were individual examples of arm switching. Division of the microRNAs according to expression level revealed that the more highly expressed half (*diamonds*) tended to have mature microRNAs predominantly from one arm, whereas the lower expressed half (*dots*) had a greater proportion of microRNAs derived from the minor arm. Several individual microRNAs of interest are named.

1% of the total number of reads (Supplementary Fig. S1B). Among these were matches to tRNAs, rRNAs, snoRNA, and small nuclear RNA (snRNA). Indeed, miR-1280 was redesignated as a tRNA-derived small RNA and removed from the latest release of miRBase.

SnoRNA-derived microRNAs

SnoRNAs are a class of small RNAs that guide modification of rRNAs, tRNAs, and snRNAs. They can be processed to generate snoRNA-derived small RNAs that resemble microRNAs.[42,43] The snoRNA ACA45 is processed by Dicer to give a well-conserved 20- to 22-nucleotide product that associates with Argonaute proteins.[44] These microRNA-like products have been termed sno-miRNAs.[45] A considerable number of reads (between 0.5% and 1.5% of all reads) in both retina and RPE/choroid mapped to a total of almost 400 different snoRNAs, although there were more in the RPE/choroid. Many reads mapping to the same snoRNAs were detected in both tissues, with SnoRD85 and SnoRD27 first and second most abundant in retina and second and third in RPE/choroid (Supplementary Tables S3A, S3B). However, reads mapping to SnoRD58 were the most abundant in RPE/choroid, 85-fold higher than in retina (Table 3, Supplementary Table S3A). Sno-miRNAs derived from all the members of the polycistronic cluster of snoRNAs located within the introns of the small nucleolar RNA host gene 1 (*Snhg1*) were detected in both retina and RPE/choroid (Fig. 6, Supplementary Table S3C).

Mirtrons

Mirtrons are a class of microRNAs that differ from canonical microRNAs in their biogenesis, which is Drosha-independent because the pre-miR from which they are processed is generated directly by the RNA splicing machinery.[46] Similar mirtrons were expressed in all samples, but at lower levels than most canonical microRNAs, the highest three in retina being miR-668, miR-1981, and miR-3102 (122, 19, and 19 reads, respectively) and in RPE/choroid uc009kyr.1, miR-3102,

Table 3. The 10 snoRNAs From Which Most Small RNAs Were Derived in Retina and RPE/Choroid

Small RNA - Name	Normalized Mean Expression Values, (RPM)
Retina	
SNORD27	426 (±29)
SNORD85	406 (±89)
SNORD57	328 (±16)
SNORD31	306 (±22)
SNORD32A	209 (±37)
SNORD45C	157 (±21)
SNORD81	145 (±4)
SCARNA17	139 (±20)
SNORD11	122 (±53)
SNORD118	122 (±15)
RPE/Choroid	
SNORD58	2971 (±377)
SNORD27	1126 (±41)
SNORD85	1051 (±17)
SNORD68	793 (±53)
SNORD81	608 (±18)
SNORD57	420 (±54)
SNORD12	405 (±91)
SNORD30	375 (±34)
SNORD25	341 (±52)
SNORD2	332 (±5)

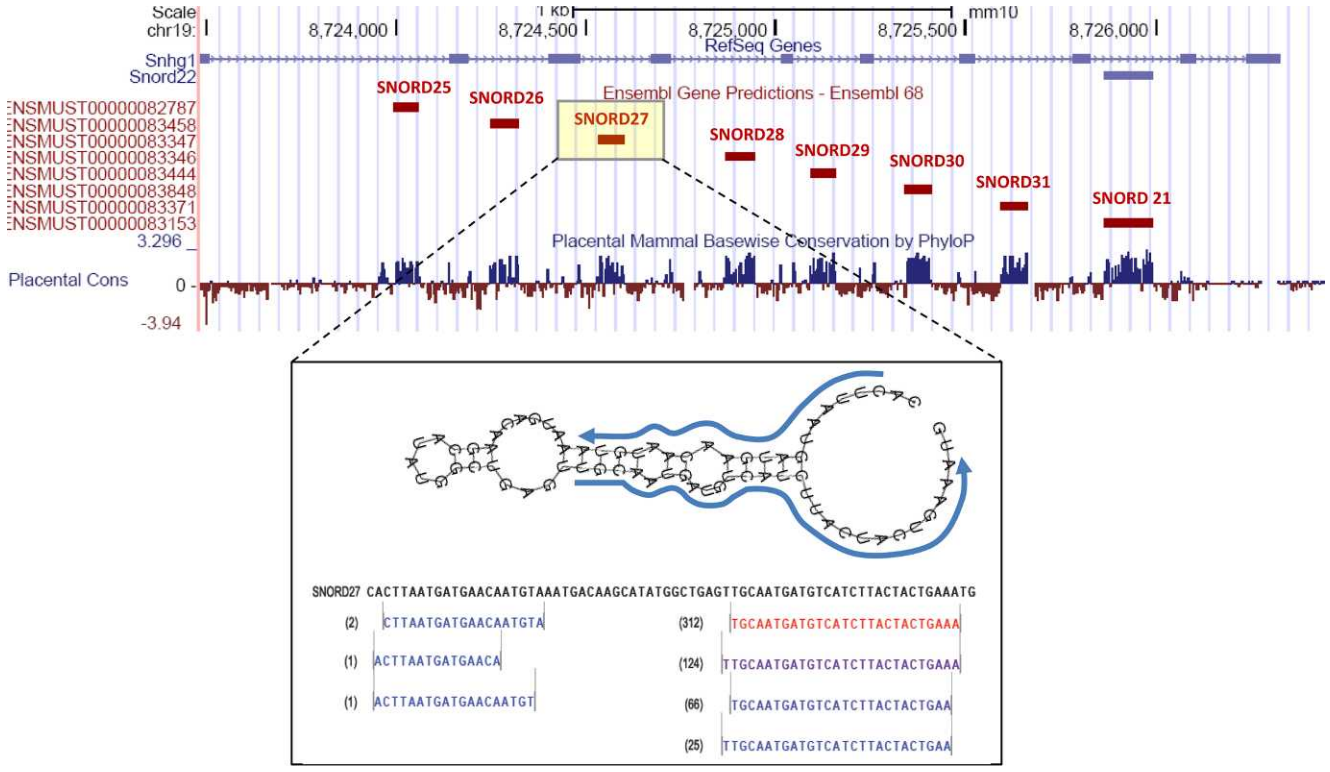

Figure 6. SnoRNAs are often transcribed as polycistronic transcripts. For example SNORD-25, -26, -27, -28, -29, -30, -31, and -21 are located in the introns of a snoRNA host gene (*Snhg1*). The snoRNAs are highly conserved among mammalian species. The sequences observed for SNORD-27 (sno-microRNAs) are mapped against the predicted secondary structure for this snoRNA.

and miR-6924 (190, 111, and 83 reads, respectively). uc009k-yr.1 is not in miRBase, but has been reported previously as a candidate mirtron.[30]

Novel microRNAs

Sequence reads that were not annotated by alignment to known mouse microRNAs in miRBase were aligned to all microRNAs from 10 other mammalian species in an attempt to detect orthologs not previously reported in mice. Three sequences present in both retina and RPE/choroid were similar to the miR-1260 family, but no plausible microRNA gene with the required stem loop structure could be identified in the mouse genome. A possible explanation for this is that they are derived from the 3′ end of a tRNA as proposed by Schopman et al.[47] for several other microRNAs; they are indeed very similar to several $tRNA_{leu}$ sequences (Supplementary Fig. S4).

Analysis using the miRTools Web server (http://centre.bioinformatics.zj.cn/mirtools/)[28] identified many putative novel microRNAs, but manual inspection revealed that most of these mapped to previously annotated ncRNAs. Two strong candidate novel microRNAs were identified among the sequences from retina; sequences from the other arm of the putative pre-miRs were also detected, an important criterion for designation of microRNAs. The novel microRNAs (named Novel_Retina1 and Novel_Retina2) are located in potential stem-loop regions with predicted minimum free energies of −56.52 and −44.50 kcal/mol, within introns of the *Mcf2l* and *Hspb6* genes (Fig. 7). Although the number of reads representing the two novel microRNAs were small (11–15), their expression in other tissues, albeit at low levels, was confirmed by analysis of publicly available small RNA sequencing data from the GEO database[29] (Supplementary Table S4). The existence of two putative novel microRNAs that overlapped snoRNA genes (named Sno_Retina1 and Sno_RPE1, Supplementary Fig. S5) was also confirmed in a range of tissues (Supplementary Table S4). The sequences have been submitted to miRBase for assignment of an accession number.

Target Predictions

To suggest some of the most important potential cellular functions regulated by microRNAs in retina and RPE/choroid, we focused on the 10 most highly expressed microRNAs in each tissue. Those microRNAs enriched more than 5-fold between the tissues, miR-181a, miR-182, and miR-183 in retina and miR-133a, miR-143, miR-22 and miR-27b in RPE/choroid, were selected. The predicted targets of these microRNAs and the pathways in which they are overrepresented were assessed by DIANAMirPath v2.0.[31] Among the four pathways significantly enriched for the combined genes predicted to be targeted by the retinal microRNAs ($P < 0.01$; Supplementary Table S5A), the neurotrophin signaling pathway ($P < 0.006$) had the most genes targeted (Fig. 8A). No pathways were significantly enriched among the predicted targets of the RPE/choroid microRNAs (Supplementary Table S5B), although several genes involved in extracellular matrix receptor interaction were targeted (*Col4a5* by miR-133a-3p and *Lamc2* by miR-22-3p).

Among the most highly expressed microRNAs (Table 2), both miR-183-5p in retina and miR-133a-3p in RPE/choroid, express abundant 5′ isomiRs (Figs. 2C, 2D). To suggest the potential functional consequences of this pattern of expression, target predictions for both the canonical mature sequence and the 5′ isomiR were performed (DIANA microT V3.0). For both microRNAs, each isomiR was predicted to target distinct genes but with some overlap (Fig. 8B). The predicted targets for both the canonical and isomiR sequences are listed in Supplementary Tables S6A and S6B.

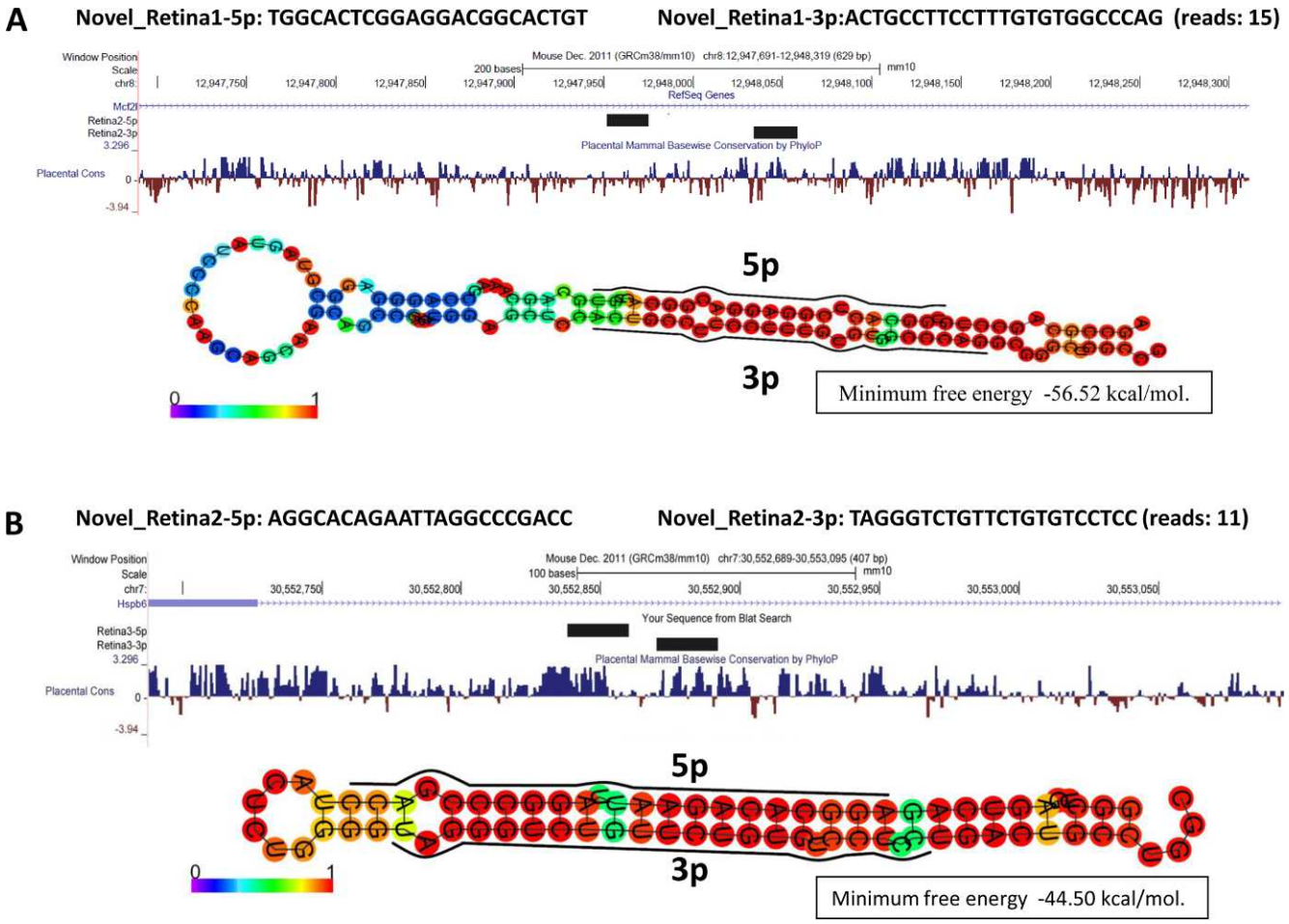

FIGURE 7. Putative novel microRNAs detected in retina mapped with the mouse genome show conservation among mammalian species and location within introns of *Mcf21* (**A**) and *Hspb6* (**B**). The putative pre-miRs have stable predicted secondary structures.

DISCUSSION

The detection of more than 300 microRNAs in both the retina and RPE/choroid demonstrates that deep sequencing is an effective approach to profile the small RNA repertoire of the retina and RPE/choroid. The sensitivity of NGS is limited primarily by read number, explaining why the only previously published data from the retina (also in C57Bl/6 mice), which contained tens of thousands rather than millions of reads, detected fewer than 250 microRNAs.[48] However, despite the use of a different platform (454; Roche) the most highly expressed microRNAs detected were consistent, with half of the top 20 most highly expressed microRNAs in the retina the same in both studies. NGS can provide greater sensitivity than microarray studies, which have detected, for example, 78 microRNAs in mouse adult retina[7] and 138 microRNAs (developing retina and in all the stages of retina, i.e., from embryonic and postnatal stages in mouse retina[3]). This is the first study to report the microRNA profile of the RPE/choroid as determined by deep sequencing.

The finding of miR-182 and miR-183 as the most highly expressed microRNAs in the retina supports their previously reported critical role in this tissue.[7,14,16,48,49] They are processed from a single polycistronic miR-183/182/96 cluster, which has been described as sensory organ specific and involved in regulation of circadian rhythm in the mouse[7] (miR-96 is the 12th most highly expressed microRNA in retina). A potential role in regulation of neuronal communication is suggested for the very highly expressed and retina-enriched microRNAs because their predicted target genes are overrepresented in the neurotrophin signaling pathway.

In the RPE/choroid, the most highly expressed microRNA is miR-143, which has previously been implicated in inhibition of several types of cancer formation and metastasis.[50–55] Of the top 10 most highly expressed microRNAs, miR-204 is perhaps the best characterized in the RPE, having been implicated in the maintenance of blood retinal barrier[56] and, together with miR-211, promoting RPE differentiations.[12]

The use of a sequencing-based approach facilitated discovery of two novel microRNAs not present in miRBase. Many small RNAs derived from snoRNAs, sometimes called "sno-miRNAs"[44] were also detected. Further reads were mapped to other classes of noncoding RNAs, underlining the complexity of the small RNA populations in both retina and RPE/choroid. It remains to be determined to what extent this complexity is reflected in individual cells or results from the combining of much less diverse RNA populations present in each of the multiple cell types present in these tissues.

NGS has revealed not only the wide range of small RNAs expressed in both the retina and RPE/choroid, but also a remarkable diversity within individual microRNAs. For every microRNA detected, multiple isoforms or isomiRs, which vary slightly in sequence, were identified. Many of these are likely to have been generated by differential processing by the RNAseIII enzymes Dicer and Drosha; the greater abundance of 5′ isomiRs in mature microRNAs derived from the 3p arm is

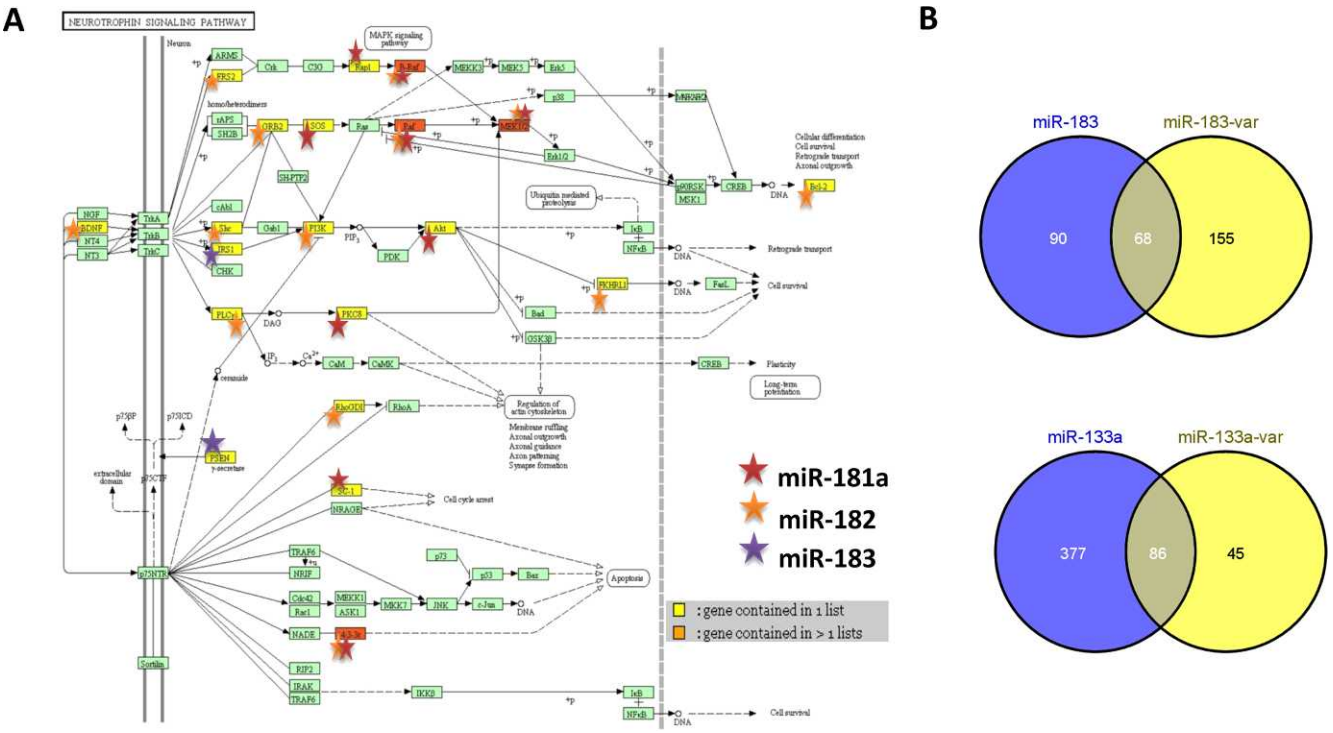

FIGURE 8. Predicted targets for top highly expressed retina and RPE/choroid enriched microRNAs and isomiRs (**A**) miR-181a-5p, -182-5p, -183-5p coordinately involved in the regulation of the neurotrophin signalling pathways. (**B**) miR-183-5p and miR-133a-3p 5′ isomiRs showed the differential targeting with some overlap in the targeting.

consistent with the previously reported lower fidelity of Dicer cleavage[38] (Fig. 1). These 5′ isomiRs differ in their seed regions from the canonical mature microRNA, which almost certainly alters their interactions with target genes. For example, the two 5′ isomiRs of miR-183 retained some predicted target genes in common, whereas many were unique to one isomiR. A similar overlap in target genes was predicted for the 5′ isomiRs of miR-133a and different functional effects have been reported for these isomiRs.[36,57]

The most common isomiRs were those exhibiting variations at the 3′ end, presumably generated by differential cleavage and possibly nuclease activity. In addition, nontemplated additions of A or T were observed, consistent with previous reports of nontemplated additions mediated by nucleotidyl transferases.[35] The functional effects of 3′ isomiRs are poorly understood, but there are specific examples of effects on stability and activity. For example, adenylation of miR-122 by the RNA nucleotidyl transferase PAPD4 increased the stability of this microRNA.[58] In contrast, uridylation of miR-26a by the RNA nucleotidyl transferase ZCCHC11 had no effect on microRNA stability, but rather reduced its ability to inhibit its mRNA target.[24]

The isomiR profiles for a specific microRNA are consistent between biological replicates of retina or RPE/choroid. However, for microRNAs present in both tissues, the isomiR profile is often distinct for each tissue. This is particularly true for microRNAs highly expressed in one of the tissues (e.g., miR-182). This suggests that different isomiRs are expressed in different cell types. This variation is not detectable by many techniques, which either do not distinguish between isomiRs or detect only the canonical sequence, as we demonstrated with the Taqman assay for miR-127-3p. Although Taqman assays have been widely used in the eye[6,7] and elsewhere to accurately measure relative microRNA expression, it is important to be aware that they do not reflect total miRNA expression and may be significantly underestimating the levels of abundant microRNAs, such as miR-127-3p.

Another source of variation for microRNA expression is the choice of arm from which the mature microRNA is derived. An intriguing phenomenon we observed was that those microRNAs for which the mature sequence was derived almost exclusively from one arm tended to be more highly expressed. Among the other microRNAs, many had significant numbers of mature microRNAs derived from each arm and in some cases the proportions varied significantly between retina and RPE/choroid.

The main conclusion of this study is that the small RNA profiles of both the retina and RPE/choroid are extremely complex. The range of functions in which microRNAs have been implicated is expanding rapidly, and although the functional roles of many of the RNA classes and variants observed in this study remain to be elucidated, it seems likely that they are significant. The differing patterns of isomiR expression observed between retina and RPE/choroid should direct future functional and expression studies to specifically target these sequences, rather than the common ones presented in miRbase and/or observed in other tissues. We must now consider the regulatory mechanisms that determine individual isomiR expression in addition to gross microRNA expression, if we wish to more fully understand the role of small RNAs in these tissues.

Acknowledgments

Supported in part by Fight for Sight (Ref 1361/62) and Biotechnology and Biological Sciences Research Council Grant BB/H005498/1. The Trinity Genome Sequencing Laboratory is a core facility funded by Science Foundation Ireland and supported by the Trinity Centre for High-Performance Computing.

Disclosure: **S.P. Soundara Pandi**, None; **M. Chen**, None; **J. Guduric-Fuchs**, None; **H. Xu**, None; **D.A. Simpson**, None

References

1. Bartel DP. MicroRNAs: genomics, biogenesis, mechanism, and function. *Cell*. 2004;116:281–297.
2. Sundermeier TR, Palczewski K. The physiological impact of microRNA gene regulation in the retina. *Cell Mol Life Sci*. 2012;69:2739–2750.
3. Hackler L Jr, Wan J, Swaroop A, Qian J, Zack DJ. MicroRNA profile of the developing mouse retina. *Invest Ophthalmol Vis Sci*. 2010;51:1823–1831.
4. Karali M, Peluso I, Gennarino VA, et al. miRNeye: a microRNA expression atlas of the mouse eye. *BMC Genomics*. 2010;11:715.
5. Karali M, Peluso I, Marigo V, Banfi S. Identification and characterization of microRNAs expressed in the mouse eye. *Invest Ophthalmol Vis Sci*. 2007;48:509–515.
6. Xu S. microRNA expression in the eyes and their significance in relation to functions. *Prog Retin Eye Res*. 2009;28:87–116.
7. Xu S, Witmer PD, Lumayag S, Kovacs B, Valle D. MicroRNA (miRNA) transcriptome of mouse retina and identification of a sensory organ-specific miRNA cluster. *J Biol Chem*. 2007;282:25053–25066.
8. Damiani D, Alexander JJ, O'Rourke JR, et al. Dicer inactivation leads to progressive functional and structural degeneration of the mouse retina. *J Neurosci*. 2008;28:4878–4887.
9. Georgi SA, Reh TA. Dicer is required for the transition from early to late progenitor state in the developing mouse retina. *J Neurosci*. 2010;30:4048–4061.
10. Iida A, Shinoe T, Baba Y, Mano H, Watanabe S. Dicer plays essential roles for retinal development by regulation of survival and differentiation. *Invest Ophthalmol Vis Sci*. 2011;52:3008–3017.
11. Walker JC. Harland RM. microRNA-24a is required to repress apoptosis in the developing neural retina. *Genes Dev*. 2009;23:1046–1051.
12. Adijanto J, Castorino JJ, Wang ZX, Maminishkis A, Grunwald GB, Philp NJ. Microphthalmia-associated transcription factor (MITF) promotes differentiation of human retinal pigment epithelium (RPE) by regulating microRNAs-204/211 expression. *J Biol Chem*. 2012;287:20491–20503.
13. Li WB, Zhang YS, Lu ZY, et al. Development of retinal pigment epithelium from human parthenogenetic embryonic stem cells and microRNA signature. *Invest Ophthalmol Vis Sci*. 2012;53:5334–5343.
14. Lumayag S, Haldin CE, Corbett NJ, et al. Inactivation of the microRNA-183/96/182 cluster results in syndromic retinal degeneration. *Proc Natl Acad Sci U S A*. 2013;110:E507–E516.
15. Loscher CJ, Hokamp K, Wilson JH, et al. A common microRNA signature in mouse models of retinal degeneration. *Exp Eye Res*. 2008;87:529–534.
16. Zhu Q, Sun W, Okano K, et al. Sponge transgenic mouse model reveals important roles for the microRNA-183 (miR-183)/96/182 cluster in postmitotic photoreceptors of the retina. *J Biol Chem*. 2011;286:31749–31760.
17. Shen J, Yang X, Xie B, et al. MicroRNAs regulate ocular neovascularization. *Mol Ther*. 2008;16:1208–1216.
18. Zhou Q, Gallagher R, Ufret-Vincenty R, Li X, Olson EN, Wang S. Regulation of angiogenesis and choroidal neovascularization by members of microRNA-23~27~24 clusters. *Proc Natl Acad Sci U S A*. 2011;108:8287–8292.
19. Wang S, Koster KM, He Y, Zhou Q. miRNAs as potential therapeutic targets for age-related macular degeneration. *Future Med Chem*. 2012;4:277–287.
20. Kozomara A, Griffiths-Jones S. miRBase: integrating microRNA annotation and deep-sequencing data. *Nucleic Acids Res*. 2011;39:D152–D157.
21. Lee Y, Kim M, Han J, et al. MicroRNA genes are transcribed by RNA polymerase II. *EMBO J*. 2004;23:4051–4060.
22. Murchison EP, Hannon GJ. miRNAs on the move: miRNA biogenesis and the RNAi machinery. *Curr Opin Cell Biol*. 2004;16:223–229.
23. Llorens F, Banez-Coronel M, Pantano L, et al. A highly expressed miR-101 isomiR is a functional silencing small RNA. *BMC Genomics*. 2013;14:104.
24. Jones MR, Quinton LJ, Blahna MT, et al. Zcchc11-dependent uridylation of microRNA directs cytokine expression. *Nat Cell Biol*. 2009;11:1157–1163.
25. Lee LW, Zhang S, Etheridge A, et al. Complexity of the microRNA repertoire revealed by next-generation sequencing. *RNA*. 2010;16:2170–2180.
26. Shi R, Chiang VL. Facile means for quantifying microRNA expression by real-time PCR. *BioTechniques*. 2005;39:519–525.
27. Pfaffl MW, Horgan GW, Dempfle L. Relative expression software tool (REST) for group-wise comparison and statistical analysis of relative expression results in real-time PCR. *Nucleic Acids Res*. 2002;30:e36.
28. Zhu E, Zhao F, Xu G, et al. mirTools: microRNA profiling and discovery based on high-throughput sequencing. *Nucleic Acids Res*. 2010;38:W392–W397.
29. Barrett T, Troup DB, Wilhite SE, et al. NCBI GEO: archive for functional genomics data sets—10 years on. *Nucleic Acids Res*. 2011;39:D1005–D1010.
30. Ladewig E, Okamura K, Flynt AS, Westholm JO, Lai EC. Discovery of hundreds of mirtrons in mouse and human small RNA data. *Genome Res*. 2012;22:1634–1645.
31. Vlachos IS, Kostoulas N, Vergoulis T, et al. DIANA miRPath v.2.0: investigating the combinatorial effect of microRNAs in pathways. *Nucleic Acids Res*. 2012;40:W498–W504.
32. Maragkakis M, Reczko M, Simossis VA, et al. DIANA-microT web server: elucidating microRNA functions through target prediction. *Nucleic Acids Res*. 2009;37:W273–W276.
33. Neilsen CT, Goodall GJ, Bracken CP. IsomiRs—the overlooked repertoire in the dynamic microRNAome. *Trends Genet*. 2012;28:544–549.
34. Bartel DP. MicroRNAs: target recognition and regulatory functions. *Cell*. 2009;136:215–233.
35. Wyman SK, Knouf EC, Parkin RK, et al. Post-transcriptional generation of miRNA variants by multiple nucleotidyl transferases contributes to miRNA transcriptome complexity. *Genome Res*. 2011;21:1450–1461.
36. Humphreys DT, Hynes CJ, Patel HR, et al. Complexity of murine cardiomyocyte miRNA biogenesis, sequence variant expression and function. *PLoS One*. 2012;7:e30933.
37. Guo L, Li H, Liang T, et al. Consistent isomiR expression patterns and 3′ addition events in miRNA gene clusters and families implicate functional and evolutionary relationships. *Mol Biol Rep*. 2012;39:6699–6706.
38. Zhou H, Arcila ML, Li Z, et al. Deep annotation of mouse iso-miR and iso-moR variation. *Nucleic Acids Res*. 2012;40:5864–5875.
39. Bortoluzzi S, Biasiolo M, Bisognin A. MicroRNA-offset RNAs (moRNAs): by-product spectators or functional players? *Trends Mol Med*. 2011;17:473–474.
40. Bortoluzzi S, Bisognin A, Biasiolo M, et al. Characterization and discovery of novel miRNAs and moRNAs in JAK2V617F-mutated SET2 cells. *Blood*. 2012;119:e120–e130.
41. Khvorova A, Reynolds A, Jayasena SD. Functional siRNAs and miRNAs exhibit strand bias. *Cell*. 2003;115:209–216.
42. Falaleeva M, Stamm S. Processing of snoRNAs as a new source of regulatory non-coding RNAs: snoRNA fragments form a new class of functional RNAs. *Bioessays*. 2013;35:46–54.

Investigative Ophthalmology & Visual Science

43. Pan YZ, Zhou A, Hu Z, Yu AM. Small nucleolar RNA-derived microrna hsa-mir-1291 modulates cellular drug disposition through direct targeting of ABC transporter ABCC1. *Drug Metab Dispos*. 2013;41:1744–1751.
44. Ender C, Krek A, Friedlander MR, et al. A human snoRNA with microRNA-like functions. *Mol Cell*. 2008;32:519–528.
45. Brameier M, Herwig A, Reinhardt R, Walter L, Gruber J. Human box C/D snoRNAs with miRNA like functions: Expanding the range of regulatory RNAs. *Nucleic Acids Res*. 2011;39:675–686.
46. Westholm JO, Lai EC. Mirtrons: microRNA biogenesis via splicing. *Biochimie*. 2011;93:1897–1904.
47. Schopman NC, Heynen S, Haasnoot J, Berkhout B. A miRNA-tRNA mix-up: TRNA origin of proposed miRNA. *RNA Biol*. 2010;7:573–576.
48. Krol J, Busskamp V, Markiewicz I, et al. Characterizing light-regulated retinal microRNAs reveals rapid turnover as a common property of neuronal microRNAs. *Cell*. 2010;141:618–631.
49. Ryan DG, Oliveira-Fernandes M, Lavker RM. MicroRNAs of the mammalian eye display distinct and overlapping tissue specificity. *Mol Vis*. 2006;12:1175–1184.
50. Akao Y, Nakagawa Y, Hirata I, et al. Role of anti-oncomirs miR-143 and –145 in human colorectal tumors. *Cancer Gene Ther*. 2010;17:398–408.
51. Hu Y, Ou Y, Wu K, Chen Y, Sun W. miR-143 inhibits the metastasis of pancreatic cancer and an associated signaling pathway. *Tumour Biol*. 2012;33:1863–1870.
52. Liu L, Yu X, Guo X, et al. miR-143 is downregulated in cervical cancer and promotes apoptosis and inhibits tumor formation by targeting bcl-2. *Mol Med Rep*. 2012;5:753–760.
53. Liu R, Liao J, Yang M, et al. The cluster of miR-143 and miR-145 affects the risk for esophageal squamous cell carcinoma through co-regulating fascin homolog 1. *PLoS One*. 2012;7:e33987.
54. Zhang Y, Wang Z, Chen M, et al. MicroRNA-143 targets MACC1 to inhibit cell invasion and migration in colorectal cancer. *Mol Cancer*. 2012;11:23.
55. Peschiaroli A, Giacobbe A, Formosa A, et al. miR-143 regulates hexokinase 2 expression in cancer cells. *Oncogene*. 2013;32:797–802.
56. Wang FE, Zhang C, Maminishkis A, et al. MicroRNA-204/211 alters epithelial physiology. *FASEB J*. 2010;24:1552–1571.
57. McGahon MK, Yarham JM, Daly A, et al. Distinctive profile of IsomiR expression and novel MicroRNAs in rat heart left ventricle. *PloS One*. 2013;8:e65809.
58. Katoh T, Sakaguchi Y, Miyauchi K, et al. Selective stabilization of mammalian microRNAs by 3′ adenylation mediated by the cytoplasmic poly(A) polymerase GLD-2. *Genes Dev*. 2009;23:433–438.

Investigative Ophthalmology & Visual Science